

# Steering Flexible Needles Under Markov Motion Uncertainty\*

Ron Alterovitz and Andrew Lim

Department of IEOR  
University of California, Berkeley  
Berkeley, CA 94720-1777, USA  
{ron,lim}@ieor.berkeley.edu

Ken Goldberg

Departments of IEOR and EECS  
University of California, Berkeley  
Berkeley, CA 94720-1777, USA  
goldberg@ieor.berkeley.edu

Gregory S. Chirikjian and Allison M. Okamura

Department of Mechanical Engineering  
The Johns Hopkins University  
Baltimore, MD 21218, USA  
{gregc,aokamura}@jhu.edu

**Abstract**—When inserted into soft tissues, flexible needles with bevel tips have been shown experimentally to follow a path of constant curvature in the direction of the bevel. By controlling 2 degrees of freedom at the needle base (bevel direction and insertion distance), these needles can be steered around obstacles to reach targets inaccessible to rigid needles. Motion planning for needle steering is a type of nonholonomic planning for a Dubins car with no reversal. We develop a motion planning algorithm based on dynamic programming where the path of the needle is uncertain due to uncertainty in tissue properties, needle mechanics, and interaction forces. The algorithm computes a discrete control sequence of insertions and direction changes so the needle reaches a target in an imaging plane while minimizing expected cost due to insertion distance, direction changes, and obstacle collisions. We efficiently sample the state space of needle tip positions and orientations and define bounds on the errors due to discretization. We formulate the motion planning problem as a Markov Decision Process (MDP) and use infinite horizon dynamic programming to compute an optimal control sequence. We first apply the method to the deterministic motion case where the needle precisely follows a path of constant curvature and then to the uncertain motion case where state transitions are defined by a probability distribution. Our implementation generates motion plans for bevel-tip needles that reach targets inaccessible to rigid needles and demonstrates that accounting for uncertainty can lead to significantly different motion plans.

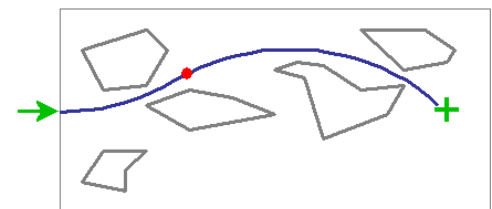
**Index Terms**—steerable needle, medical robotics, nonholonomic motion planning, dynamic programming, Markov decision process.

## I. INTRODUCTION

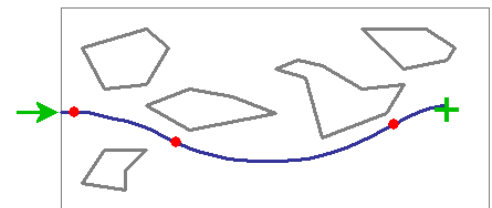
Many diagnostic and therapeutic medical procedures require insertion of a needle to a specific location in soft tissue, including biopsy to obtain a tissue sample for testing, drug treatment injections for anesthesia, or radioactive seed implantation for brachytherapy cancer treatment. Unlike traditional rigid needles, highly flexible bevel-tip needles can be steered around obstacles by taking advantage of needle bending and the asymmetric forces applied by the needle tip to the tissue [18], [19], [1]. This steering capability allows flexible bevel-tip needles to reach targets inaccessible to traditional rigid needles.

Planning motions for such needles is difficult due to nonholonomic constraints, particularly in the case with uncertainty in the motion due to the biological variability between

\*This work was supported in part by the National Institutes of Health under grant R21 EB003452 and a National Science Foundation Graduate Research Fellowship to Ron Alterovitz.



(a) Steerable needle plan assuming deterministic motion



(b) Steerable needle plan assuming uncertain motion

Fig. 1. Needle must be inserted at left and must reach target (centered at “+”) inside the body without touching critical areas indicated by polygonal obstacles in the imaging plane. The motion planner computes a sequence of insertions and direction changes (indicated by dots) to steer the needle to the target. In the deterministic motion case (a), the needle precisely follows a path of constant curvature in the bevel-left or bevel-right direction. In the uncertain motion case (b), the expected needle path is drawn for a needle whose orientation after each insertion is uncertain and is distributed as defined in section VI. The control sequence computed in the uncertain motion case results in a path with more direction changes but greater clearance from the obstacles to account for the probability of collision due to needle tip orientation uncertainty.

humans. In this paper we develop a motion planning algorithm for steerable bevel-tip needle insertion in an imaging plane that considers uncertainty in the needle’s response to control.

The feasible workspace for motion planning is defined by the region of tissues through which the needle can be steered. Obstacles represent tissues that cannot be cut by the needle, such as bone, or sensitive tissues that should not be damaged, such as nerves or arteries. The workspace and obstacles can be specified by segmenting a 2D cross-section of the patient anatomy obtained using medical imaging such as ultrasound or MRI. Although volumetric MR images can be constructed by stacking multiple planar slices, the inter-slice distance is significantly greater than the diameter of a medical needle. In this paper we consider motion plans in an imaging plane.

Steerable bevel-tip needles are controlled by 2 degrees of freedom actuated at the needle base: insertion distance and rotation angle about the needle axis. Insertion pushes the

needle deeper into the tissue while rotation re-orient the bevel at the needle tip. For a sufficiently flexible needle, rotating the needle base will change the bevel direction without changing the needle’s position in the tissue. In the plane, the needle base can be rotated  $180^\circ$  about the insertion axis so the bevel points in either the bevel-left or bevel-right direction. When inserted, the asymmetric force applied by the needle tip causes the needle to bend and follow an arc through the tissue, which we assume is stiff relative to the needle. It was shown experimentally by Webster et al. that a flexible bevel-tip needle inserted into a stiff tissue phantom cuts a path of constant curvature in the direction of the bevel and the needle shaft bends to follow the path cut by the bevel tip [18].

The steerable needle motion planning problem is to determine a sequence of controls (insertions and direction changes) so the needle tip reaches the specified target while avoiding obstacles and staying inside the workspace. In the absence of uncertainty, the path followed by the needle is subject to the nonholonomic constraint of constant curvature in the bevel-left or bevel-right direction. This is equivalent to a Dubins car that cannot drive in reverse and is additionally constrained to only steer its wheels far left or far right. To minimize tissue damage, insertion time, and errors, shorter needle paths with fewer direction changes are preferred.

In this paper we develop a planner that formulates the motion planning problem as a Markov Decision Process (MDP) using a discretization of space and orientation and computes an optimal discrete sequence of controls using dynamic programming. We consider both the deterministic motion case (where the needle response to controls is known with certainty) and the uncertain motion case (where the probability distribution of responses to controls is known). Like a well-constructed navigation field, the motion planner provides an optimal control for any state in the workspace. However, the planner is not complete; it may not find a feasible solution when one exists due to discretization error. The output of our implementation is shown for a sample case in Fig. 1 and demonstrates that considering uncertainty during planning results in substantially different motion plans for steerable needles.

## II. RELATED WORK

Webster et al. show experimentally that steerable bevel-tip needles follow paths of constant curvature in the direction of the bevel tip [18]. The radius of curvature of the needle is not significantly affected by insertion velocity [19]. Webster et al. also develop a nonholonomic model of steerable bevel-tip needle motion in stiff tissues based on a generalization of the bicycle model and fit model parameters using experiments on tissue phantoms [18].

Nonholonomic motion planning has a long history in robotics and related fields [11], [12]. Past work has addressed deterministic curvature-constrained path planning where a mobile robot is constrained to follow a path of minimum turning radius [7], [10], [16]. Dubins showed that the optimal

curvature-constrained trajectory in open space from a start pose to a target pose can be described from a discrete set of canonical trajectories composed of straight line segments and arcs of minimum radius of curvature [7]. Jacobs and Canny consider obstacles and construct a configuration space for a set of canonical trajectories [10]. Sellen’s representation of orientation by appropriate discretization of a unit circle for a Dubins path inspired our discretization approach [16]. Our planning problem considers steerable needles that have *constant* magnitude turning radius with cost for direction changes rather than following a path constrained by a *minimum* turning radius. In the limiting case of zero cost for direction changes, previously developed algorithms for deterministic curvature-constrained Dubins paths can be applied because the needle can be rotated continuously as it is inserted to approximate a straight line segment in the path.

Park et al. formulate the planning problem for steerable bevel-tip needles in stiff tissue as a nonholonomic kinematics problem based on a 3D extension of a unicycle model and use a diffusion-based motion planning algorithm to numerically compute a path [14]. The approach is based on recent advances by Zhou and Chirikjian in nonholonomic motion planning including stochastic model-based motion planning to compensate for noise bias [21] and probabilistic models of dead-reckoning error in nonholonomic robots [20]. Park’s method searches for a feasible path in full 3D space using continuous control but does not consider obstacle avoidance, although the authors plan to address this limitation. The method does not handle uncertainty of the response of the needle to insertion or direction change controls. In this paper, we develop a 2D motion planning approach for bevel-tip needle insertion under uncertainty to generate paths to a target based on discrete controls that minimize expected cost incurred due to obstacle collisions, insertion distance, and direction changes.

Past work has investigated needle insertion planning in situations where soft tissue deformations are significant and can be modeled. Our past work addressed planning optimal insertion location and insertion distance for rigid symmetric-tip needles to compensate for 2D tissue deformations [2], [3]. Past work has also addressed steering slightly flexible symmetric-tip needles by translating and orienting the needle base to explicitly cause tissue deformations that will guide the needle around point obstacles with oval-shaped potential fields [6]. Glozman and Shoham also address symmetric-tip needles and approximate the tissue using springs [9]. We previously developed a different 2D planner to explicitly compensate for the effects of tissue deformation by combining finite element simulation with numeric optimization [1]. This previous approach assuming that bevel direction can only be set once prior to insertion and uses local optimization that will fail to find a globally optimal solution in the presence of obstacles.

Medical needle insertion procedures may benefit from the more precise control of needle position and velocity made possible through robotic surgical assistants. A survey of recent

advances in medical robotics was written by Taylor and Stoianovici [17]. Dedicated hardware for needle insertion is being developed for stereotactic neurosurgery [13], MR compatible surgical assistance [5], and prostate biopsy and therapeutic interventions [8], [15].

### III. PROBLEM DEFINITION

A bevel-tip needle, unlike a symmetric-tip needle, will cut tissue at an angle, as shown in Fig. 2. We assume uniform soft tissue that is stiff relative to the needle, so the tissue does not deform significantly. When inserted into soft tissue, the steerable bevel-tip needle will follow a path of constant curvature [18] with radius of curvature  $r$ , which is a property of the needle and tissue. In 2D, the direction of the bevel  $b$  is either bevel-left ( $b=0$ ) or bevel-right ( $b=1$ ). We only consider insertion, not retraction, of the needle.

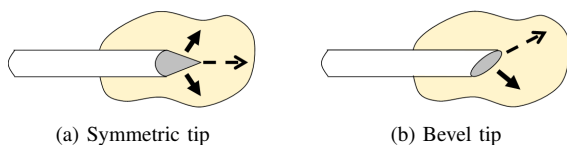


Fig. 2. A symmetric-tip needle exerts forces on the tissue equally in all directions, so it cuts tissue in the direction that the tip is moving. A bevel-tip needle exerts forces asymmetrically and cuts tissue at an offset angle depending on the tissue properties and bevel angle.

We define the workspace as a 2D rectangle of depth  $z_{max}$  and height  $y_{max}$ . We do not consider motion by the needle out of the imaging plane. Obstacles in the workspace are defined by (possibly nonconvex) polygons. The target region is defined by a point  $\mathbf{t}$  and radius  $r_t$ .

We assume the needle is controlled at discrete intervals because needle rotation causes tissue damage and to allow verification of the needle tip direction since the tip may not rotate by the same angle as the base due to imperfect torsional stiffness of the needle shaft. In our model, direction changes can only occur at discrete *control points*, which are separated by an insertion distance of  $\delta$ . One of two actions  $u$  can be selected at any control point: insert the needle a distance  $\delta$  ( $u = 0$ ) or change direction (rotate the bevel  $180^\circ$ ) and insert a distance  $\delta$  ( $u = 1$ ). We assume the needle insertion velocity is 0 during rotation and that the needle is inserted at constant positive velocity between rotations.

Because needle insertion can damage living tissues, cost  $C_i$  is incurred for every unit length that the needle is inserted. Cost  $C_r$  is incurred every time the needle is rotated since this may also damage tissues and requires additional time. A prohibitive cost  $C_o$  is incurred when the needle collides with an obstacle and  $C_e$  when the needle exits the workspace.

The needle's initial state is defined by a point  $\mathbf{s}$ , orientation  $\theta_0$ , and bevel direction  $b_0$ . A feasible plan is a sequence of discrete controls  $U = [u_0, u_1, \dots]$  that steers the needle along a path from the initial state to the target without intersecting an obstacle. Every control  $u = 1$  in  $U$  incurs an additional cost  $C_r$ .

The goal of needle insertion planning is to generate a feasible plan  $U$  that minimizes cost  $J$ , where  $J$  is a weighted sum

of the costs, as defined formally below for the deterministic and uncertain motion cases.

### IV. PROBLEM FORMULATION

The state of the needle during insertion is fully characterized by the position  $\mathbf{p} = (p_y, p_z)$  of the needle tip, the orientation angle  $\theta$  of the needle tip, and the bevel direction  $b$ , as shown in Fig. 3.

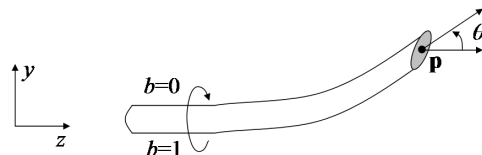


Fig. 3. The state of a bevel-tip needle during insertion is characterized by the tip position  $\mathbf{p}$ , tip orientation angle  $\theta$ , and the bevel direction  $b$ . In this figure,  $b = 0$  (bevel-left) and the needle tip is following a constant curvature path in the counter-clockwise direction.

Our motion planning algorithm based on dynamic programming requires a discrete representation of state. To make this approach viable, we must round  $\mathbf{p}$  and  $\theta$  without generating an unwieldy number of states while simultaneously minimizing error due to discretization.

#### A. Discrete State Space

Our discretization of the planar workspace is based on a grid of points with a spacing  $\Delta$  horizontally and vertically. We approximate a point  $\mathbf{p} = (p_y, p_z)$  by rounding to the nearest point  $\mathbf{q} = (q_y, q_z)$  on the grid. For a rectangular workspace bounded by depth  $z_{max}$  and height  $y_{max}$ , this results in

$$N_s = \frac{z_{max}y_{max}}{\Delta^2}$$

position states.

Appropriate discretization of orientation is critical to avoid an explosion of the number of states and large discretization error. For example, defining one state for each degree of  $\theta$  for each grid position would result in  $360N_s$  states and an orientation error of up to  $0.5^\circ$ . This orientation error would propagate and compound after each state transition. Instead, we take advantage of discrete insertion distances to develop a more efficient method for representing orientation.

We define a *control circle* of radius  $r$ , the radius of curvature of the needle. Each point  $\mathbf{c}$  on the control circle represents an orientation  $\theta$  of the needle, where  $\theta$  is the angle of the tangent of the circle at  $\mathbf{c}$  with respect to the  $z$ -axis. If  $b = 0$ , the needle will trace an arc of length  $\delta$  along the control circle in a counter-clockwise direction. If  $b = 1$ , the needle will trace an arc in a clockwise direction. If control  $u = 1$ , the needle is rotated  $180^\circ$  to change bevel direction. On the control circle, this action corresponds to rotating the point  $\mathbf{c}$  representing the needle tip by  $180^\circ$  to the other side of the circle and tracing subsequent insertions on the control circle in the opposite direction, as shown in Fig. 4.

We subdivide the control circle into  $N_c$  equally sized arcs of length  $\delta = 2\pi r/N_c$ , the needle insertion distance between

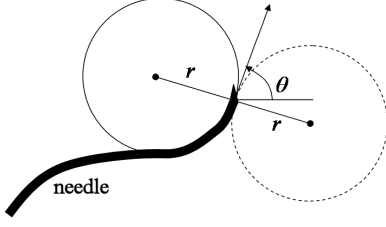


Fig. 4. The needle, currently in the  $b = 0$  bevel-left direction, is tracing the solid control circle with radius  $r$  in the counter-clockwise direction. The needle orientation  $\theta$  is the tangent angle of the control circle. If the bevel direction is changed to the  $b = 1$  bevel-right direction, the needle will begin to trace the dashed control circle in the clockwise direction at a tangent point  $180^\circ$  from its tangent point on the solid control circle.

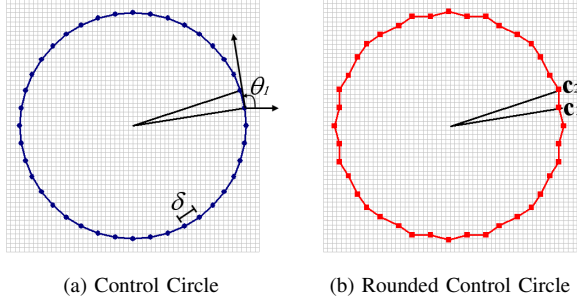


Fig. 5. The control circle is subdivided into  $N_c = 40$  discrete arcs of length  $\delta$ , the insertion distance between controls (a). Control circle point 1 corresponds to a needle orientation  $\theta_1$ . The control circle points are rounded to the nearest point on the  $\Delta$ -density grid (b). If the needle is at orientation  $\theta_1$  and is inserted a distance  $\delta$ , the displacement of the needle tip will be  $\mathbf{c}_2 - \mathbf{c}_1$ .

controls. The endpoints of the arcs generate a set of  $N_c$  control circle points,  $\mathbf{c}_i$ ,  $i = 0, \dots, N_c - 1$ , each representing a discrete orientation state, as shown in Fig. 5(a). We require that  $N_c$  is a multiple of 4 to facilitate the orientation state change after a bevel direction change.

We overlay the control circle on a regular grid of spacing  $\Delta$  and round the positions of the control circle points  $\mathbf{c}_i$  to the nearest grid point, as shown in Fig. 5(b). The vector  $\mathbf{c}_{i+1} - \mathbf{c}_i$  represents the displacement of the needle tip in the space of the  $N_s$  grid points for orientation  $i$  and bevel direction  $b = 0$ . Similarly,  $\mathbf{c}_{i-1} - \mathbf{c}_i$  represents the displacement of the needle tip for orientation  $i$  and bevel direction  $b = 1$ . We compute and store all  $N_c$  orientation vectors so we can quickly trace the needle path as a function of the bevel direction  $b$  for every control interval of length  $\delta$ . As discussed in section V-B, this discretization results in 0 discretization error in orientation when the needle is controlled at  $\delta$  intervals.

Using this formulation, our state defined by position  $\mathbf{p} = (p_y, p_z)$ , orientation  $\theta$ , and bevel direction  $b$  can be approximated as a discrete state by  $s = \{\mathbf{q}, \Theta, b\}$ , where  $\mathbf{q} = (q_y, q_z)$  is the discrete point closest to  $\mathbf{p} = (p_y, p_z)$  on the  $\Delta$ -density grid, and  $\Theta$  is the integer index to the discrete control circle orientation whose corresponding arc includes tangent angle  $\theta$ . The total number of discrete states is

$$N = 2N_s N_c = \frac{4\pi r z_{max} y_{max}}{\Delta^2 \delta}.$$

There are two types of special states: target states and obstacle states. A state  $s = \{\mathbf{q}, \Theta, b\}$  is a target state if  $\mathbf{q}$  is inside the target circle of radius  $r_t$  centered at  $\mathbf{t}$ . Any state  $s = \{\mathbf{q}, \Theta, b\}$  is considered an obstacle state if the point  $\mathbf{q}$  is inside an obstacle polygon.

### B. State Transitions

The transition probability matrix  $P_{ij}(u)$  specifies the probability of transitioning from state  $i$  to state  $j$  when control  $u$  is applied. Target states are cost-free termination states and transition to themselves with probability 1 regardless of the control  $u$ . Obstacle states transition to a termination state with probability 1 since the needle can no longer proceed. Transition probabilities for the remaining states depend on the uncertainty of needle motion.

In the deterministic motion case, the response of a needle to a control  $u$  is known with certainty. The successor state  $m$  to state  $i$  is a function of  $i$  and  $u$  and is determined by the grid and control circle defined in section IV-A. Hence,  $P_{im}(u) = 1$  and  $P_{ij}(u) = 0$  for all  $j \neq m$ .

In the uncertain motion case, the successor state  $m$  to state  $i$  is not a deterministic function of state  $i$  and control  $u$ . Instead, a probability distribution is defined for state  $m$ . However, state  $m$  must be a distance  $\delta$  from  $i$  (within discretization error) and the bevel direction of state  $m$  must equal the bevel direction of state  $i$  if  $u = 0$  and must be unequal otherwise. We discuss our current implementation of the transition probability matrix in section VI.

The cost  $g$  of a transition is a function of current state  $i$ , control  $u$ , and next state  $j$ . If state  $i$  is a target state, then the next state  $j$  must also be a target state and the cost  $g(i, u, j)$  is 0. If state  $i$  is not a target state and the path from  $i$  to  $j$  does not cross an obstacle, then

$$g(i, u, j) = C_i \delta + \begin{cases} 0 & \text{if } u = 0 \\ C_r & \text{if } u = 1 \end{cases}$$

where cost is incurred both for distance inserted  $\delta$  and the cost of direction change (if any). If the arc from state  $i$  to state  $j$  intersects an edge of a polygonal obstacle, then cost  $C_o$  is incurred and the system transitions to a termination state. In our implementation, we approximate the arc between states by a line segment and check if the segment intersects an edge of any obstacle polygon. Similarly, a cost  $C_e$  is incurred if the arc starting at state  $i$  exits the workspace.

### C. Total Cost

For a given sequence of controls  $U = [u_0, u_1, \dots]$  and initial state  $x_0$ , the total cost  $J(x_0)$  is the expected value of the sum of the transition costs.

$$\begin{aligned} J(x_0) &= E \left[ \sum_{k=0}^{\infty} g(x_k, u_k, x_{k+1}) \right] & (1) \\ &= \sum_{k=0}^{\infty} \sum_{x_{k+1}=1}^N P_{x_k x_{k+1}}(u_k) g(x_k, u_k, x_{k+1}) & (2) \end{aligned}$$

## V. MOTION PLANNING OPTIMIZATION

The goal of the planner is to compute a sequence of controls  $U$  that minimizes  $J(x_0)$ , the total expected cost of inserting a steerable bevel-tip needle to a target. This problem has the form of a stochastic shortest path problem, which can be optimally solved using infinite horizon dynamic programming [4]. The Bellman equation for this problem is:

$$J^*(i) = \min_u E [g(i, u, j) + J^*(j)] \quad (3)$$

$$= \min_u \sum_{j=1}^N P_{ij}(u) (g(i, u, j) + J^*(j)). \quad (4)$$

The system transitions as a Markov Decision Process (MDP).

### A. Dynamic Programming

We use value iteration [4] to solve the dynamic programming problem defined by the Bellman equation (4). If deterministic motion is assumed, the formulation is equivalent to a deterministic shortest path problem and termination of value iteration is guaranteed [4]. In general, termination is guaranteed in  $N$  iterations if the transition probability graph corresponding to some optimal stationary policy is acyclic [4]. Violation of this requirement will be rare in motion planning since it implies that an optimal control sequence results in a path that, with probability greater than 0, loops and passes through the same point at the same orientation more than once. In our implementation, we terminate value iteration when the maximum change  $\epsilon$  over all states is less than  $10^{-3}$ , which generally occurs in far fewer than  $N$  iterations.

To improve performance, we take advantage of the sparsity of the matrices  $P_{ij}(u)$  for  $u = 0$  and  $u = 1$ . Since there are  $N$  states, the matrix  $P_{ij}(u)$  has  $N^2$  entries. However, each row of  $P_{ij}(u)$  has only  $k$  nonzero entries, where  $k \ll N$  since the needle will only transition to a state  $j$  in the spatial vicinity of state  $i$ . Hence,  $P_{ij}(u)$  has only  $kN$  nonzero entries. The deterministic motion case is a special case where  $k = 1$ . We represent the  $P_{ij}(u)$  matrices using an array of size  $N$ , where row  $m$  of the array points to a list of the nonzero entries for the row  $m$  of  $P_{ij}(u)$ . By only accessing nonzero entries of  $P_{ij}(u)$  during computation, each iteration of the value iteration algorithm requires only  $O(kN)$  rather than  $O(N^2)$  time and memory.

### B. Discretization Error

The paths generated by the planner are not precise due to error incurred during discretization of the state space.

In the deterministic motion case, the needle is always inserted a distance  $\delta$  and the orientation of the needle can be precisely computed and stored by calculating the angle of the tangent of the (continuous) control circle at the insertion distance of the needle tip. However, at any control point  $\mathbf{p}$ , the error between the approximated point  $\mathbf{q}$  on the workspace grid and the real point  $\mathbf{p}$  is  $E_1 = \Delta\sqrt{2}/2$ , half the distance between two diagonal grid points. If the needle follows a constant curvature path and is never rotated, the final needle position error is bounded by  $E_1$ . However, every time the

bevel direction is changed, the position error at the time of the direction change becomes permanent because the center of the original control circle and the center of the control circle after the direction change will be a distance in the range  $2r \pm \Delta\sqrt{2}$  apart. Hence, for a needle path with  $k$  direction changes, the final orientation is precise but the error in position is bounded above by

$$E_k = k\Delta\sqrt{2} + \Delta\sqrt{2}/2 = \frac{\Delta\sqrt{2}}{2} (2k + 1).$$

In the uncertain motion case, additional error is incurred due to the discretization of the probability distribution into states. This error depends on the probability distribution.

Another related source of error is the control distance  $\delta$ . A constant curvature path may exist between a given start pose and end pose when  $\delta \rightarrow 0$  but may not exist when  $\delta$  is finite.

## VI. COMPUTATIONAL RESULTS

We implemented the motion planner in C++ and tested it on a 1.6GHz Pentium M laptop. We set the needle radius of curvature  $r = 5.0$ . The workspace is defined by  $z_{max} = 10$  and  $y_{max} = 5$ . The workspace discretization is defined by parameters  $N_c = 100$ ,  $\Delta = z_{max}/N_c = 0.1$  and  $\delta = 2\pi r/N_c = 0.313$ . Transition cost parameters were set to  $C_i = 1$ ,  $C_r = 10$ ,  $C_o = 1000$ ,  $C_e = 100$ . The resulting dynamic programming problem contained  $N = 1,000,000$  states.

In our current implementation of the uncertain motion case, we model uncertainty due to tissue inhomogeneity that introduce noise into the needle tip orientation. We assume 80% probability that the needle follows the deterministic path, 10% probability that the needle orientation is increased by  $3.6^\circ$  (one transition along the control circle), and 10% probability that the needle orientation is decreased by  $3.6^\circ$ . These probabilities were selected for testing purposes; we plan to perform physical experiments to obtain accurate estimates of the transition probabilities in future work.

The output of the method is shown in Fig. 1 for a test case containing 5 polygonal obstacles. The path in the uncertain motion case has a greater clearance from the obstacles and workspace boundary to avoid obstacle collision and exit penalties when the needle deviates from the expected path. However, the needle cannot deviate too far into the free space and still reach the target region because of the large radius of curvature of the needle relative to the workspace.

The uncertain motion solution requires 3 direction changes whereas the deterministic motion solution requires only 1 direction change. As a consequence, the final discretization error of 0.17 for the uncertain motion solution is greater than the discretization error of 0.15 for the deterministic motion solution. The expected needle path based on a constant curvature response to the computed control sequence of insertions and direction changes differs from the approximate needle path based on the discrete states used in the planner algorithm, as shown in Fig. 6. The deterministic motion solution required 26 seconds of computation time to build the data structures and terminate after 44 value iterations. The uncertain motion solution required 58 seconds and 51 value iterations.

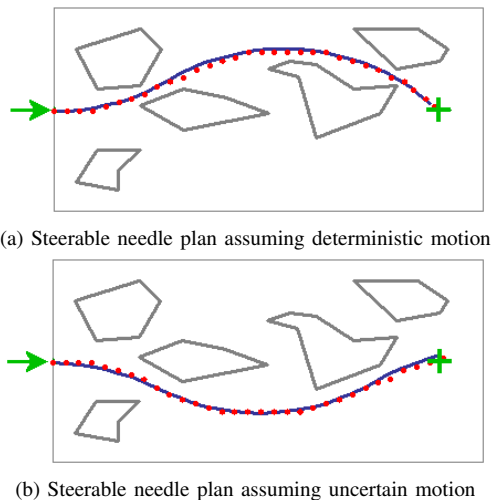


Fig. 6. The solid line shows the expected needle path based on a constant curvature response to the computed control sequence of insertions and direction changes. The dotted line shows the approximate needle path based on the discrete states used in the planner algorithm. Errors due to discretization are smaller in the deterministic motion solution because the bevel direction changes fewer times.

## VII. CONCLUSION

We develop a motion planning algorithm for bevel-tip steerable needles that computes a discrete control sequence of insertions and direction changes so the needle path avoids polygonal obstacles and reaches a target on a 2D imaging plane. We define the state space by a regular grid of points, an efficient discretization of needle orientation, and bevel direction. We formulate the motion planning problem as a Markov Decision Process (MDP) and compute an optimal sequence of controls using infinite horizon dynamic programming.

In the deterministic motion case, the needle precisely follows a path of constant curvature. In the uncertain motion case, state transitions are based on a probability distribution. We observe that computed motion plans in the uncertain motion case stay further away from obstacles and the workspace boundary than paths in the deterministic motion case. Intuitively this is expected because the large cost of colliding with an obstacle or exiting the workspace, even weighted by a small probability, is greater than the costs incurred inserting the needle with more direction changes or along a longer path.

We implemented the motion planner in C++ and ran a test problem of 1,000,000 states shown in Fig. 1 on a 1.6GHz Pentium M laptop. The method required 26 seconds to compute the deterministic motion solution and 58 seconds for the uncertain motion case. While this performance is adequate for grid dimensions of 50 by 100 with 100 discrete orientations, we hope to decrease computation requirements to allow interactive applications or larger state spaces with smaller discretization errors. In future work, we plan to improve performance by considering alternatives to the value iteration method and investigate the state transition probability distributions using physical experiments.

## ACKNOWLEDGMENT

We thank Russ Taylor for introducing us to the problem of needle insertion and Robert Webster, Dezhen Song, A. Frank van der Stappen, and K. Gopalakrishnan for their valuable feedback and assistance. We also thank physicians Leonard Shlain of CPMC and I-Chow Hsu of UCSF for their feedback on medical aspects of this work.

## REFERENCES

- [1] R. Alterovitz, K. Goldberg, and A. Okamura, "Planning for steerable bevel-tip needle insertion through 2D soft tissue with obstacles," in *Proc. IEEE Int. Conf. on Robotics and Automation*, Apr. 2005, pp. 1652–1657.
- [2] R. Alterovitz, J. Pouliot, R. Taschereau, I.-C. Hsu, and K. Goldberg, "Needle insertion and radioactive seed implantation in human tissues: Simulation and sensitivity analysis," in *Proc. IEEE Int. Conf. on Robotics and Automation*, vol. 2, Sept. 2003, pp. 1793–1799.
- [3] —, "Sensorless planning for medical needle insertion procedures," in *Proc. IEEE/RSJ Int. Conf. on Intelligent Robots and Systems*, vol. 3, Oct. 2003, pp. 3337–3343.
- [4] D. P. Bertsekas, *Dynamic Programming and Optimal Control*, 2nd ed. Athena Scientific, 2000.
- [5] K. Chinzei, N. Hata, F. A. Jolesz, and R. Kikinis, "MR compatible surgical assist robot: System integration and preliminary feasibility study," in *MICCAI*, 2000.
- [6] S. P. DiMaio and S. E. Salcudean, "Needle steering and model-based trajectory planning," in *MICCAI*, 2003.
- [7] L. Dubins, "On curves of minimal length with a constraint on average curvature and with prescribed initial and terminal positions and tangents," *American Journal of Mathematics*, vol. 79, pp. 497–516, 1957.
- [8] G. Fichtinger, T. L. DeWeese, A. Patriciu, A. Tanacs, D. Mazilu, J. H. Anderson, K. Masamune, R. H. Taylor, and D. Stoianovici, "System for robotically assisted prostate biopsy and therapy with intraoperative CT guidance," *Academic Radiology*, vol. 9, no. 1, pp. 60–74, 2002.
- [9] D. Glozman and M. Shoham, "Flexible needle steering and optimal trajectory planning for percutaneous therapies," in *MICCAI*, Sept. 2004.
- [10] P. Jacobs and J. Canny, "Planning smooth paths for mobile robots," in *Proc. IEEE Int. Conf. on Robotics and Automation*, May 1989.
- [11] J.-C. Latombe, *Robot Motion Planning*. Kluwer Academic Pub., 1991.
- [12] —, "Motion planning: A journey of robots, molecules, digital actors, and other artifacts," *International Journal of Robotics Research*, vol. 18, no. 11, pp. 1119–1128, Nov. 1999.
- [13] K. Masamune, L. Ji, M. Suzuki, T. Dohi, H. Iseki, and K. Takakura, "A newly developed stereotactic robot with detachable drive for neurosurgery," in *MICCAI*, 1998.
- [14] W. Park, J. S. Kim, Y. Zhou, N. J. Cowan, A. M. Okamura, and G. S. Chirikjian, "Diffusion-based motion planning for a nonholonomic flexible needle model," in *Proc. IEEE Int. Conf. on Robotics and Automation*, Apr. 2005, pp. 4611–4616.
- [15] C. Schneider, A. M. Okamura, and G. Fichtinger, "A robotic system for transrectal needle insertion into the prostate with integrated ultrasound," in *Proc. IEEE Int. Conf. on Robotics and Automation*, May 2004, pp. 2085–2091.
- [16] J. Sellen, "Approximation and decision algorithms for curvature-constrained path planning: A state-space approach," in *Workshop on the Algorithmic Foundations of Robotics (WAFR)*, 1998, pp. 59–67.
- [17] R. H. Taylor and D. Stoianovici, "Medical robotics in computer-integrated surgery," *IEEE Transactions on Robotics and Automation*, vol. 19, no. 5, pp. 765–781, Oct. 2003.
- [18] R. J. Webster III, N. J. Cowan, G. Chirikjian, and A. M. Okamura, "Nonholonomic modeling of needle steering," in *Proc. 9th International Symposium on Experimental Robotics*, June 2004.
- [19] R. J. Webster III, J. Memisevic, and A. M. Okamura, "Design considerations for robotic needle steering," in *Proc. IEEE Int. Conf. on Robotics and Automation*, Apr. 2005, pp. 3599–3605.
- [20] Y. Zhou and G. S. Chirikjian, "Probabilistic models of dead-reckoning error in nonholonomic mobile robots," in *Proc. IEEE Int. Conf. on Robotics and Automation*, Sept. 2003, pp. 1594–1599.
- [21] —, "Planning for noise-induced trajectory bias in nonholonomic robots with uncertainty," in *Proc. IEEE Int. Conf. on Robotics and Automation*, Apr. 2004, pp. 4596–4601.